

Two tone response in Superconducting Quantum Interference Filters

P. Caputo, J. Tomes, J. Oppenländer, Ch. Häussler, A. Friesch, T. Träuble, and N. Schopohl

Abstract— We successfully exploit the parabolic shape of the dc voltage output dip around $B = 0$ of a Superconducting Quantum Interference Filter (SQIF) to mix weak external rf signals. The two tone response of weak time harmonic electromagnetic fields has been detected on the spectral voltage output of the SQIF at frequency $f_0 = f_1 - f_2$, for various frequencies f_1 and f_2 ranging from few MHz up to 20 GHz. The two tone response is a characteristic function of static magnetic field B and of bias current I_b , related to the second derivative of the dc voltage output.

Index Terms— SQIF, arrays, Josephson junctions, rf .

I. INTRODUCTION

SUPERCONDUCTING Quantum Interference Filters (SQIFs), when operated in the resistive mode, have been shown to be effective flux-to-voltage transformers with a high transfer factor [1], [2] and large voltage swing. Employing various flux focusing structures together with a SQIF it is possible to further significantly enhance the transfer factor [3], [4].

In the presence of incident time dependent electromagnetic fields, the spectral voltage output $\hat{V}(I_b, B, f)$ of a SQIF is the Fourier transform of the voltage $V(I_b + i_{rf}(t), B + b_{rf}(t), t)$. The dependence of the coupling strength of the incident rf signals depends on the bias current I_b and the static field B . It can be estimated for slowly varying signals as

$$\begin{aligned} & \left\langle V(\overbrace{I_b + i_{rf}(t)}^{\text{bias coupling}}, \underbrace{B + b_{rf}(t)}_{\text{flux coupling}}, t) \right\rangle = \\ & = V_{dc}(I_b, B) + (i_{rf}(t) \partial_{I_b} + b_{rf}(t) \partial_B) V_{dc}(I_b, B) \\ & + \frac{1}{2} (i_{rf}(t) \partial_{I_b} + b_{rf}(t) \partial_B)^2 V_{dc}(I_b, B) + \dots \end{aligned} \quad (1)$$

Here $V_{dc}(I_b, B)$ is the dc voltage output of the SQIF in the absence of any incident rf signals; ∂_{I_b} and ∂_B denote the partial derivatives with respect to I_b and B , respectively. The fluctuation $i_{rf}(t)$ of the bias current describes the response to the incident electric field $e_{rf}(t)$.

In recent work [5], we investigated the two tone response of the SQIF to weak time harmonic rf magnetic fields $b_{rf}(t) = b_{rf1} \cos(2\pi f_1 t) + b_{rf2} \cos(2\pi f_2 t)$, in a frequency range up to a few hundred MHz.

In the following we study the response of the SQIF to weak time harmonic rf electromagnetic fields $b_{rf}(t)$ and $e_{rf}(t)$

P. Caputo, J. Tomes, J. Oppenländer, Ch. Häussler, A. Friesch, and T. Träuble are with QUEST, Quantenelektronische Systeme GmbH, Steigackerstr. 13, 72768 Reutlingen (Germany).

N. Schopohl is with Lehrstuhl für Theoretische Festkörperphysik, Universität Tübingen, Auf der Morgenstelle 14, 72076 Tübingen (Germany).

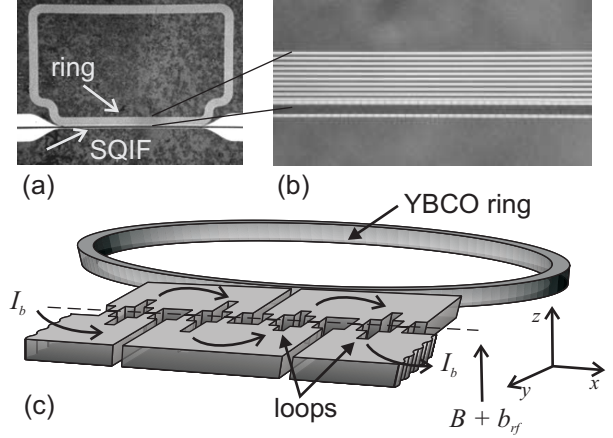


Fig. 1. (a) Optical microscope image of the chip with the SQIF placed along the grain boundary, and the superconducting ring inductively coupled to the SQIF; (b) zoom on the ring made of 10 equidistant parallel loops, one aligned inside the other. All superconducting parts, except the regions across the junctions, are covered by gold. (c) Sketch, not in scale, of the SQIF-sensor; the dashed line represents the grain boundary; the meandered path of the bias current and the direction of the magnetic field are shown by arrows.

consisting of two tones in the frequency range from few MHz up to 20 GHz. The two tone response is studied as a function of static magnetic field B and of bias current I_b .

II. TWO TONE EXPERIMENTS

A. The setup

Our SQIFs are manufactured from $\text{YBa}_2\text{Cu}_3\text{O}_{7-x}$ grain boundary Josephson junctions grown on 24° -oriented bicrystal MgO substrates [6]. The junction width is $2\mu\text{m}$, the $\text{YBa}_2\text{Cu}_3\text{O}_{7-x}$ layer is 130 nm thick, so that the resulting junction critical current density is $J_c \approx 23\text{ kA/cm}^2$, at $T = 77\text{ K}$. The SQIF consists of 211 loops biased in series, the distribution of the loop areas ranging between $38\mu\text{m}^2$ and $210\mu\text{m}^2$. The wirings connecting the loops in series form a meandered path across the grain boundary, as sketched in Fig. 1(c). In order to provide flux focusing, we fabricated a SQIF with a superconducting ring, placed at one side of the grain boundary and inductively coupled to the SQIF. Figure 1(a) is an optical microscope image of the SQIF-sensor. The focusing loop is effectively a split loop design, consisting of 10 equidistant parallel thin loops, one aligned inside the other; calculations show [7] that the split ring design leads, in average, to a larger current density compared to a single ring of the same cross section. With the split ring, we have achieved an enhanced sensitivity to the magnetic field, *i.e.* a

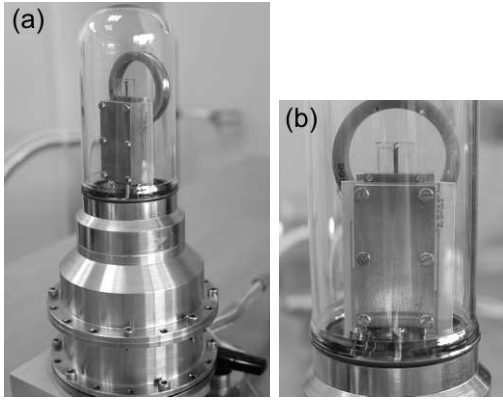


Fig. 2. Experimental setup with the cryocooler and the glass dewar (a); enlarged view of the chip and of the amplifier (b). The chip is anchored by one side at the cold finger and coupled to the amplifier by a coplanar line. Directly under the chip, the multi-turn coil is mounted, for the static field B .

larger transfer factor $V_B = \max(\partial V / \partial B)$. A fragment of the split ring is in Fig. 1(b).

The static magnetic field B is applied via a multi-turn coil placed inside the dewar; the rf magnetic field $b_{rf}(t)$ is broadcast by a $50\ \Omega$ -loop antenna (outside the dewar). For the two tone experiments, the rf field is a superposition of two time harmonic signals, applied to the loop antenna by means of two independent generators. The experiments presented here were made with a mu-metal shield surrounding the dewar; the loop antenna was placed inside the shield, at a distance of about 5 cm from the chip.

Samples have been operated in a Stirling microcooler [8], at temperatures from 55 to 82 K. To provide transparency to the rf fields, a glass chamber surrounds the microcooler cold head. Figure 2 shows the typical experimental setup. The sample is anchored to the cold head only from one side, in order to keep the focusing ring as much as possible free of metallic ground plane. On the cold head, an rf amplifier is also mounted, designed for cryogenic applications with a bandwidth $0.04 - 6$ GHz. At room temperature and at the typical bias values, we have measured a noise figure of the amplifier of about 1 dB, in the frequency range $0.1 - 1$ GHz. The SQIF is coupled to the amplifier through a coplanar line, after which a bias-Tee is placed. The bias-Tee splits the rf and the dc signals: the rf , through a capacitor, goes to the first stage of the amplifier; the dc signal (bias input & voltage output), through a conical inductor, goes to the room temperature electronics, via twisted wires. The amplifier output is carried outside the cooler via an SMA feed-through, and detected by a spectrum analyzer.

The two tone experiments are performed in the following way. The rf fields at frequencies f_1 and f_2 are broadcast. The spectrum analyzer is operated in *Zero Span Mode*, i.e. as a narrowband receiver tuned at the central frequency f_0 (equal to the frequency at which the detection of the SQIF spectral voltage output is made, i.e. the mixed frequency $f_0 = f_1 - f_2$), and with a bandwidth around f_0 set by the Resolution Bandwidth (ResBW). To this mode, there corresponds an analog output proportional to the maximum amplitude of the signal at f_0 . This output voltage is recorded by computer while slowly

sweeping either the static magnetic field B (simultaneously, the $V_{dc}(B)$ - curve is acquired), or sweeping the static bias current I_b (simultaneously, the $V_{dc}(I_b)$ - curve is acquired).

B. Two tone response on the SQIF $V_{dc}(B)$ - curve

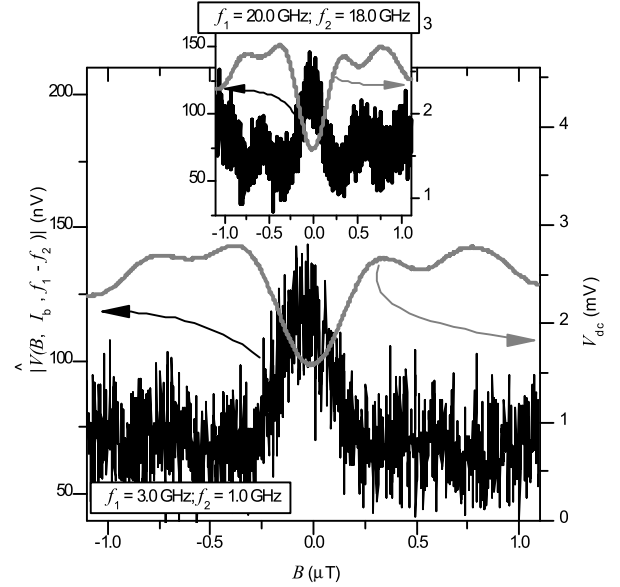


Fig. 3. The two incident signals are set at $f_1 = 3.0$ GHz and $f_2 = 1.0$ GHz. Gray curve, relative to right axis: V_{dc} vs. B ; black curve, rel. to left axis: spectral voltage $|\hat{V}(B, I_b, f)|$ detected at $f_0 = f_1 - f_2 = 2.0$ GHz. Inset (axis title and scale as in the figure): $f_1 = 20.0$ GHz, $f_2 = 18.0$ GHz, and $f_0 = 2.0$ GHz. For both plots: $I_b = 20\ \mu\text{A}$ & $T = 73$ K; ResBW is 30 kHz.

We first measure the $V_{dc}(B)$ dependence of the SQIF at a constant I_b value, and check the dip symmetry with respect to zero magnetic field. At $T \approx 73$ K and at $I_b = 20\ \mu\text{A}$, we measure a voltage span $\Delta V \approx 1280\ \mu\text{V}$ and a transfer factor $V_B \approx 5500\ \text{V/T}$. The SQIF normal resistance is $R = 250\ \Omega$. Successively, the rf is switched ON: a time harmonic signal which is the superposition of two rf signals with frequencies f_1 and f_2 and equal amplitudes b_{rf1} and b_{rf2} is applied to the primary antenna, while the rf output of the SQIF is detected. A small amplitude of the incoming signals is required, so that the rf signal superimposed to the static field does not modulated the SQIF working point out of the dip and corrupt the effect; but it has to be high enough so that the SQIF spectral voltage output is above the noise level set by the resolution bandwidth (ResBW) of the spectrum analyzer. The analog output of the spectrum analyzer is recorded by computer while slowly sweeping the static field B (sweep frequency in the kHz range); simultaneously, the dc voltage output V_{dc} is acquired as a function of B . In the output spectra, we find the component at $f_0 = |f_1 - f_2|$, whose amplitude is maximal at the dip bottom and vanishes in the region of zero curvature of the $V_{dc}(B)$ curve. Indeed, the amplitude of the second harmonics (the term in $f_1 - f_2$) is expected to be proportional to the curvature in the $\partial_B^2 V_{dc}|_{I_b}$. Naturally, the SQIF spectral voltage contains also harmonics at f_1 and at f_2 , with the amplitude dependence proportional to the slope $\partial_B V_{dc}|_{I_b}$, as reported in [5]. We have detected the two tone response of incident

fields at frequencies up to 20 GHz (upper limit of our signal generators), keeping the difference frequency f_0 within the bandwidth of the *rf* amplifier. Figure 3 and its inset display the typically measured curves. The incident field is a linear combination of two signals with frequencies $f_1 = 3.0$ GHz and $f_2 = 1.0$ GHz, and equal amplitudes (-24 dBm). In the spectral voltage output of the SQIF, we find the component at the difference frequency $f_0 = 2.0$ GHz, and in the Figure is displayed the spectral voltage output $|\hat{V}(B, I_b, f)|$ detected at the central frequency f_0 , with $\text{ResBW} = 30$ kHz, as a function of the sweeping parameter B . The bias current was $I_b = 20 \mu\text{A}$, and $T = 73\text{K}$. Around $f_0 = 2.0$ GHz, the gain of the amplifier is about 40 dB. The amplitude of the spectral voltage output is maximal around $B = 0$, and vanishes as the dc working point approaches the dip slopes; eventually, in other regions of the $V_{\text{dc}}(B)$ -curve with non-zero curvature, the detected spectral voltage rises again from the noise level. In the inset of Fig. 3 is reported the same type of measurement, with the following parameters: the incident fields are at $f_1 = 20.0$ GHz and $f_2 = 18.0$ GHz (amplitudes -15 dBm); the detection is made at $f_0 = 2.0$ GHz, with $\text{ResBW} = 30$ kHz. As one can see, the two tone response is also present for incoming signals with larger frequencies. Indeed, we have detected the quadratic harmonics over a broad frequency range: for incident fields from a few hundred MHz up to 20 GHz, keeping their distance at various constant values suitable for the bandwidth of our amplifier (within 100MHz – 6GHz). Qualitatively, no significant changes were observed, over the entire frequency range. A part from the levels of the output signals, which systematically tend to lower at higher frequencies.

C. Two tone response on the SQIF $V_{\text{dc}}(I_b)$ - curve

At $B = 0$, the $V_{\text{dc}}(I_b)$ curve is swept; the two incident *rf* signals are applied to the primary antenna, and the spectral voltage output of the SQIF sensor is detected. To the applied time harmonic magnetic field, there corresponds naturally a time harmonic electric field, which couples to the SQIF voltage output through the fluctuations induced in the bias current (if we assume the electric field to have a component parallel to the bias line). Thus, the spectral voltage output detected vs. I_b might also contain fingerprints of the incident signals, and eventually mix them. Figure 4 and its inset display the typically measured curves. The incident field is a linear combination of two signals with frequencies $f_1 = 3.0$ GHz and $f_2 = 1.9$ GHz, and amplitudes -44 dBm. In the spectral voltage output of the SQIF, we find the quadratic mixing component at $f_0 = f_1 - f_2 = 1.1$ GHz, detected with a ResBW of 3 kHz. Also in this case, the amplitude of the voltage output at $f_1 - f_2$ is found to be maximal around the region of maximal curvature of the $V_{\text{dc}}(I_b)$ - characteristics. In the inset of Fig. 4 is reported the same type of measurement, with the following parameters: the incident fields are generated at $f_1 = 18.0$ GHz and $f_2 = 13.0$ GHz, with amplitudes -14 dBm; the detection is made at $f_0 = 5.0$ GHz, with $\text{ResBW} = 3$ kHz. In contrast to the case of the $V_{\text{dc}}(B)$ -curve, when sweeping the $V_{\text{dc}}(I_b)$ -curve the spectral voltage output contains a component at $f_0 = 2f_2 - f_1$,

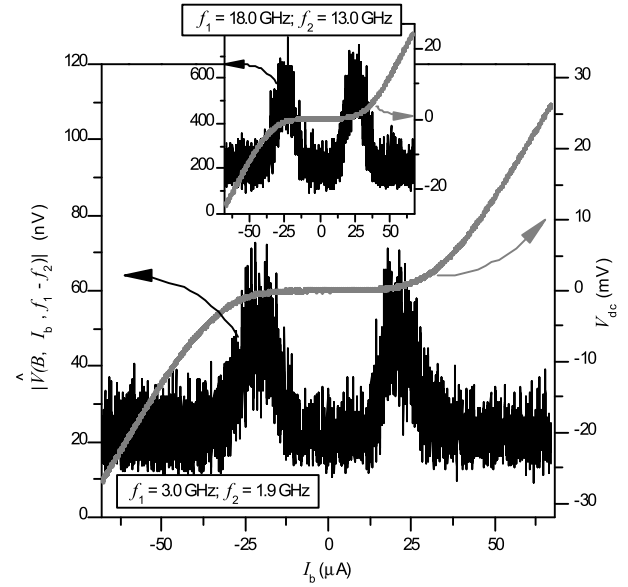


Fig. 4. The two incident signals are set at $f_1 = 3.0$ GHz and $f_2 = 1.9$ GHz. Gray curve, relative to right axis: V_{dc} vs. I_b , at $B = 0$; black curve, rel. to left axis: spectral voltage $|\hat{V}(B, I_b, f)|$ detected at $f_0 = f_1 - f_2 = 1.1$ GHz; Inset (axis title and scale as in the figure): $f_1 = 18.0$ GHz, $f_2 = 13.0$ GHz, and $f_0 = 5.0$ GHz. For both plots, the ResBW is 3 kHz, and $T = 73.5$ K.

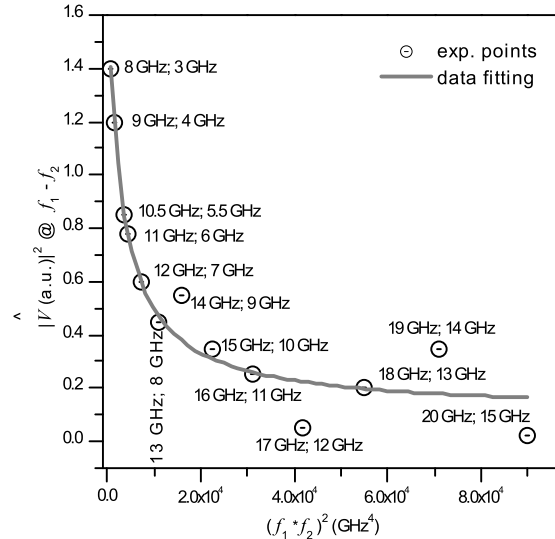


Fig. 5. Maximum power levels of the spectral component detected at $f_0 = f_1 - f_2 = 5.0$ GHz, for various frequencies of the two incident signals of constant amplitudes (-40 dBm), and plotted (circles) as a function of the squared product of the corresponding frequencies. The power levels were taken in the region of maximum curvature of the $V_{\text{dc}}(I_b)$ -curve. For all points, ResBW is 3 kHz. The data fitting (continuous line) is $\propto (f_1 \cdot f_2)^{-2}$.

with an amplitude dependence proportional to the third order derivative of the $V_{\text{dc}}(I_b)$ -curve [11].

D. Frequency dependence of the two tone response on the $V_{\text{dc}}(I_b)$ - curve

We have analyzed the amplitude of the two tone response vs. frequency of the incident fields, keeping constant the difference frequency f_0 . Over the whole frequency range, the two fields were broadcast with constant amplitudes equal to

-40 dBm. This does not necessary imply that the SQIF-sensor was irradiated with constant energy, since the efficiency of the primary antenna depends on frequency. The two tone response *vs.* frequency was measured on the $V_{dc}(I_b)$ - curve. As pointed out in the previous section, the presence of the two tone response when sweeping the $V_{dc}(I_b)$ - curve might be ascribed to the voltage fluctuations induced by the rf electric field via coupling to the bias current. In Fig. 5, the y-axis represents, for a given pair of incident fields broadcast at f_1 and f_2 , the maximum amplitude of the spectral component detected at the difference frequency $f_0 = 5\text{GHz}$. Since the directly measured amplitude is in fact the power level $[\propto V^2]$ of the spectral component at f_0 , the data are plotted as a function of the *square* of the product of the two frequencies $[(f_1 \cdot f_2)^2]$. The data fitting, made with a function proportional to $(f_1 \cdot f_2)^{-2}$, well describes the set of experimental points. As can be demonstrated, in the presence of an *rf* electric field which is a linear combination of two fields at f_1 and f_2 , and which couples to the *dc* bias current by adding dispersive fluctuations, the spectral voltage output $V(I_b + i_{rf}(t))$ at $f_1 - f_2$ has a $(f_1 \cdot f_2)^{-1}$ -dependence in the prefactor. Thus, in Fig. 5 the observed dependence on frequency of the power levels of the spectral component detected at f_0 *vs.* the squared frequency product $(f_1 \cdot f_2)^2$ is yet another evidence of the electric bias coupling to the applied electromagnetic fields. The observed dependence on frequency reflects the $1/\omega$ dependence of the conductivity $\sigma(\omega)$ in a superconductor. The strength of this coupling is comparable to that of the magnetic coupling (induced by the time dependent magnetic flux threading the SQIF loops at the rate of the incident fields).

III. CONCLUSIONS

We have studied the two tone response of Superconducting Quantum Interference Filters over a frequency range from few MHz to 20 GHz. Incident *rf* fields couple either through the time dependent magnetic flux threading the loops of the interferometer, or through the bias current, so that the response arises both on the $V_{dc}(B)$ - and $V_{dc}(I_b)$ -curves. The experiments reveal independence of the two tone response on the sweeping parameter, either B or I_b , irrespective of the frequency of the individual tones f_1 and f_2 . This is expected if one trusts a determination of the Josephson frequency from an estimation of the noise-free critical current, which gives a value around 40 GHz for our JJ's [12]. When the two tone response arises on the $V_{dc}(I_b)$ - curve, its voltage amplitude as a function of the frequencies of the incident *rf* fields decays as $1/(f_1 \cdot f_2)$, confirming that the broadcast electromagnetic fields couple to the SQIF not only through the time dependent magnetic flux threading the loops, but also through the voltage fluctuations induced by the bias current fluctuations due to the time dependent electric field.

ACKNOWLEDGMENTS

The authors would like to acknowledge many useful discussions with R. IJsselsteijn and V. Schultze.

REFERENCES

- [1] J. Oppenländer, Ch. Häussler, and N. Schopohl, Phys. Rev. B, **63**, 024511 (2000).
- [2] Ch. Häussler, J. Oppenländer, and N. Schopohl, J. Appl. Phys., **89**, 1875 (2001).
- [3] V. Schultze, R. IJsselsteijn, R. Boucher, H.-G. Meyer, J. Oppenländer and Ch. Häussler, and N. Schopohl, Supercond. Sci. Technol., **16**, 1356 (2003).
- [4] V. Schultze, R. IJsselsteijn and H.-G. Meyer, Supercond. Sci. Technol., **19**, 411 (2006).
- [5] P. Caputo, J. Tömes, J. Oppenländer, Ch. Häussler, A. Friesch, T. Träuble, and N. Schopohl, Appl. Phys. Lett., **89**, 062507 (2006).
- [6] Institute for Physical High Technology (IPHT), Jena, Germany.
- [7] F. Ludwig, A. B. M. Jansman, D. Drung, M. O. Lindström, S. Bechstein, J. Beyer, J. Flokstra, and T. Schurig, IEEE Trans. Appl. Supercond., **11**, 1315 (2001).
- [8] AIM, AEG Infrarot-Module GmbH, Heilbronn, Germany.
- [9] J. Oppenländer, Ch. Häussler, A. Friesch, J. Tömes, P. Caputo, T. Träuble, and N. Schopohl, IEEE Trans. Appl. Supercond., **15**, 936 (2005).
- [10] P. Caputo, J. Oppenländer, Ch. Häussler, J. Tömes, A. Friesch, T. Träuble, and N. Schopohl, Appl. Phys. Lett., **85**, 1389 (2004).
- [11] P. Caputo, J. Tömes, J. Oppenländer, Ch. Häussler, A. Friesch, T. Träuble, and N. Schopohl, accepted for publication in J. Supercond. (as proceeding of HTSHFF Symposium, Cardiff 2006)
- [12] R. IJsselsteijn and V. Schultze, private communication.